
SEAMLESS MONITORING OF STRESS LEVELS LEVERAGING A UNIVERSAL MODEL FOR TIME SEQUENCES

Davide Gabrielli

Computer Science Department
Sapienza University of Rome
gabrielli.1883616@studenti.uniroma1.it

Bardh Prenkaj*

Computer Science Department
Sapienza University of Rome
prenkaj@di.uniroma1.it

Paola Velardi†

Computer Science Department
Sapienza University of Rome
velardi@di.uniroma1.it

ABSTRACT

Monitoring the stress level in patients with neurodegenerative diseases can help manage symptoms, improve patient’s quality of life, and provide insight into disease progression. In the literature, ECG, actigraphy, speech, voice, and facial analysis have proven effective at detecting patients’ emotions. On the other hand, these tools are invasive and do not integrate smoothly into the patient’s daily life. HRV has also been proven to effectively indicate stress conditions, especially in combination with other signals. However, when HRV is derived from less invasive devices than the ECG, like smartwatches and bracelets, the quality of measurements significantly degrades. This paper presents a methodology for stress detection from a smartwatch based on a universal model for time series, UniTS, which we fine-tuned for the task. We cast the problem as anomaly detection rather than classification to favor model adaptation to individual patients and allow the clinician to maintain greater control over the system’s predictions. We demonstrate that our proposed model considerably surpasses 12 top-performing methods on 3 benchmark datasets. Furthermore, unlike other state-of-the-art systems, UniTS enables seamless monitoring, as it shows comparable performance when using signals from invasive or lightweight devices.

Keywords Anomaly Detection · Seamless Monitoring · Foundation Models · Transformers · Neurodegenerative Diseases · Stress Detection

1 Introduction

High stress levels can worsen the symptoms of neurodegenerative diseases such as Alzheimer’s and Parkinson’s [22]. In these patients, stress is generated by mood changes such as depression and apathy, confinement at home, and other factors such as social isolation, uncertainty about the evolution of the disease, and the economic, health, personal, and family situation [23] [18]. Analyzing stress levels can provide insights into disease progression and help healthcare providers adjust treatment plans accordingly. Managing stress can also improve patients’ quality of life and help to inform new therapeutic strategies.

AI-based methods for stress detection are motivated by the need for early, timely, and personalized stress management solutions. These methods leverage cutting-edge machine learning algorithms to provide objective, real-time monitoring and analysis, significantly contributing to the field of mental health and well-being (see, among others, [40]).

*He is also with the Chair of Responsible Data Science at the Technical University of Munich.

†Corresponding author.

Among the numerous techniques presented in the literature, those based on data extracted from sensor devices are particularly promising due to several advantages. One of the key benefits of using sensor-based methods is their ability to provide real-time data, which is crucial for timely interventions and stress management. Secondly, they protect privacy more than solutions based on behavioral signals such as speech, gestures, and facial expressions [26], a particularly relevant aspect for elderly and frail people. Third, they may support continuous monitoring, enabling more convenient home care solutions for patients and caregivers.

In the literature, various sensor types are used to detect stress, leveraging different physiological signals. As surveyed in [36], commonly used devices are ECG and EDA, EEG, skin temperature, respiratory and pressure sensors, and activity sensors like accelerometers, gyroscopes, and RFID technology. Among these devices, only a few are well-suited for seamless monitoring due to factors such as invasiveness, lack of autonomy for patients, and high costs. We define *seamless* monitoring as the real-time collection of signals that is i) without time limits, ii) uninterrupted, and iii) does not require explicit actions by patients and/or doctors³. In other terms, while continuous monitoring only ensures that data is captured without interruption, seamless monitoring ensures that this process integrates smoothly into the patient’s daily life. To address this challenge, which is essential to facilitate the widespread adoption of monitoring technologies for stress detection and healthcare applications in general, we propose a methodology providing the following contributions:

1. To detect stress signals from sensor data, we leverage for the first time a universal model for time sequences, UniTS [12], achieving 9% superior performance against the best performing – i.e., MSCRED [39] – among 12 compared state-of-the-art (SoTA) methods on 3 publicly available datasets;
2. The proposed model allows us to obtain, using data from lightweight devices, performances comparable to those obtained from more invasive devices, such as ECG, thus enabling seamless monitoring;
3. We cast the problem of stress detection as anomaly detection rather than classification, as the majority of works in the literature do (see Table 1). Anomaly detection typically involves establishing a baseline of normality rather than learning boundaries between multiple classes. The former is a more straightforward process since any deviation from normal behavior can be visualized and investigated for specific reasons. This way, doctors can more easily understand and trust the system’s predictions, thereby enhancing their ability to provide high-quality care.
4. We release our code publicly⁴ with all the model weights to encourage reproducibility from future researchers.

2 Related Work

Our work relates to the fields of AI-based emotion monitoring from sensor data and anomaly detection from time series.

	Signals Used	Application	Device Type	Model Type	Task	Year
[44]	ECG	S	ECG Wearable	Conv. Gaussian Mixture VAE	AD	2023
[2]	Temp., Humidity (Sweat), Steps	S	Wristband	Stacked Ens. with GB	C	2023
[8]	HR, GSR, Acc	S	Smartwatch	MLP	C	2019
[14]	Resp., GSR, HR, EMG	S	*	SVM, kNN	C	2015
[15]	BVP, HR, ST, GSR, Resp.	S	Smartwatch	RF	C	2017
[32]	Steps, Acc	S	Wristband	SVM, kNN	C	2013
[24]	GSR (+ Speech)	S	GSR Device	SVM	C	2013
[1]	EEG, ECG	S	Wearable	SVM	C	2019
[7]	HR	E	Wristband	SVM, kNN, RF	C	2021
[16]	HRV (from ECG)	E	ECG Wearable	SVM	C	2016
[17]	SpO2, Pulse Rate	E	Pulse Oximetry	SVM	C	2018
[21]	ECM, ECG, GSR, Resp.	E	*	pLDA	C	2008
[27]	HR, BP	E	Smartwatch	Fuzzy Petri Net [9]	C	2021
[us]	HRV, HR	S + E	Smartwatch ECG	Transformer	AD	2024

Table 1: Organization of the literature on ML methods for mood monitoring from physiological data.

³In this sense, ECG is not seamless, because it can usually last for 24-48 hours, and must be activated by the doctor or patient, depending upon the device type.

⁴<https://github.com/davegabe/Wearable-Stress-Monitor>

2.1 Emotion Monitoring and Stress Detection

Table 1 summarizes the key details regarding research on emotion recognition through physiological signals, providing a qualitative comparison with the solution proposed in this paper. (1) “*Signals Used*” lists the physiological signals employed. Examples are Electrocardiogram (ECG), Heart Rate (HR), Galvanic Skin Response (GSR), Respiration (Resp.), and Electromyogram (EMG), among others. The choice of signals is crucial as it directly affects the accuracy and reliability of the detection system. Different signals provide varied information about an individual’s physiological state, impacting the performance of the employed models. (2) “*Application*” specifies whether the study focuses on stress (S) or emotion (E) detection, whereas the second considers more nuanced mental conditions. (3) “*Device Type*” specifies the type of device used to collect the physiological signals, such as wearables, smartwatches, wristbands, GSR devices, or pulse oximetry. The device type influences the monitoring system’s accuracy, practicality, comfort, and user acceptance. Only some types of devices allow for seamless monitoring in real-world settings, which is especially valuable for frail people. (4) “*Model Type*” lists the machine learning or statistical models used for classification tasks. Notice how, with the exception of [2] and [44], all works rely on simple off-the-shelf machine learning models (SVM, kNN, and pLDA⁵), which might not be suitable to detect emotions or stress levels that are not in the training data distribution, and therefore have limited capacity for generalization but also for personalization. In [2], an ensemble mechanism over Gradient Boosts (GB) is applied to classify stress levels by leveraging the expertise of multiple models. In this case, a linear regression meta-model is applied to the output of the GB base models to predict the final outcome. In [44], a clustering algorithm based on a Gaussian mixture convolutional variational autoencoder is employed to identify normal emotional patterns and detect anomalies. *To the best of our knowledge, we are the first to use a state-of-the-art Transformer model to tackle stress and abnormal emotion detection.* (5) “*Task*” indicates whether the model’s task is classification (C) or anomaly detection (AD). Most works tackle stress and emotion monitoring as classification problems, categorizing states into predefined classes. The only exception is UAED [44], which performs an anomaly detection task. We argue that approaching stress monitoring as an anomaly detection problem is more principled and inherently more explainable than doing fine-grained emotion classification.

2.2 Anomaly Detection in Time Series

Following [44], we cast stress monitoring as a problem of anomaly detection. We identified five categories of methods proposed in the literature for anomaly detection in time series. Distance-based outlier detectors consider the distance of a point from its k-nearest neighbors. Density-based methods (among others [38, 35]) consider the density of the point and its neighbors. Prediction-based methods (among others, [5]) calculate the difference between the predicted and true values to detect anomalies. Reconstruction-based methods (among others [11]) compare the input signal and the reconstructed one in the output layer, typically using autoencoders. These methods assume anomalies are difficult to reconstruct and lost when the signal is mapped to lower dimensions, so a higher reconstruction error indicates a higher anomaly score.

Recently, GANs have been employed for anomaly detection in time series data. MAD-GAN [25] combines the discriminator output and reconstruction error to detect anomalies in multivariate time series. BeatGAN [43] uses an encoder-decoder generator with a modified time-warping-based data augmentation to detect anomalies in medical ECG inputs. TadGAN [13] uses a cycle-consistent GAN architecture with an encoder-decoder generator and proposes several ways to compute reconstruction error combined with critic outputs. HypAD [11] proposes using hyperbolic uncertainty for anomaly detection. Tuli et al. [37] introduce TranAD, built on deep transformer networks. This model leverages attention-based sequence encoders to infer broader temporal patterns within the data. TranAD employs focus score-based self-conditioning to enhance its performance for effective multi-modal feature extraction and utilizes adversarial training to ensure stability. Finally, Zhu et al. [44] rely on a 2d Convolutional Variational Autoencoder with a Gaussian Mixture Model as the latent representation distribution. Interestingly, the authors extrapolate ECG signals, stack them vertically on top of one another, and process them as images to detect anomalies unsupervisedly.

In this paper, we employ for the first time a foundation multi-task model specialized for time series, UniTS [12], showing that it considerably surpasses best-performing anomaly detection models, including GAN, in the task of stress detection from physiological signals.

3 Method

UniTS [12] is the first foundation model⁶ for multivariate time series, designed to perform in a unified way various tasks such as forecasting, imputation, classification, and anomaly detection. It employs self-attention to capture relationships

⁵Extended Linear Discriminant Analysis.

⁶foundation models are pre-trained on broad data at scale and can be adapted to a wide range of downstream tasks.

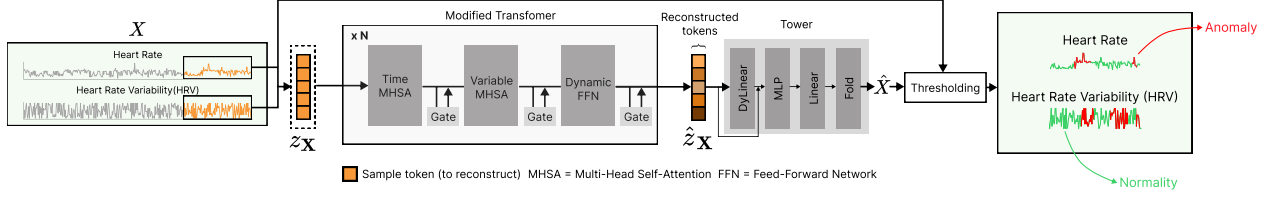


Figure 1: Finetuning of the UniTS architecture for anomaly detection. The multivariate time series in input gets transformed into several tokens, which are then passed through N different blocks of the UniTS model. UniTS reconstructs the sample tokens, which are unpatched and compared against the real tokens. The comparison uses a dynamic threshold to discern between anomalies and normality. For visualization purposes, we do not illustrate the prompt tokens concatenated to the sample ones.

across both the sequence and variable dimensions. This is particularly beneficial in our multi-sensor domain since if one variable has an anomaly, the model can assess how this anomaly correlates with the patterns observed in other variables, thereby improving detection accuracy. Furthermore, UniTS is designed to integrate signals of different types and lengths in a cohesive manner. To achieve this, it employs multi-scale processing techniques to handle time-series data of different lengths, which involves processing the data at various temporal resolutions.

3.1 Problem Definition and Preliminaries

Anomaly detection in multivariate time series [4, 11, 31] is the process of identifying observations within a sequence of time-dependent multivariate data that deviate significantly from the learned patterns of normal behavior. Formally, consider a multivariate time series $\mathbf{X} = \{\mathbf{x}_1, \mathbf{x}_2, \dots, \mathbf{x}_T\}$, where $\mathbf{x}_t \in \mathbb{R}^n$ represents the n -dimensional observation at time t , and T is the total number of time points. The objective is to develop a model f based on a historical subset of data $\mathbf{X}_{train} = \{\mathbf{x}_1, \mathbf{x}_2, \dots, \mathbf{x}_t\}$ for $t < T$, that captures the normal behavior of the series.

For each time point t , an anomaly score $S_t = g(\mathbf{x}_t, f(\mathbf{X}_{train}))$ is computed, where g measures the deviation of \mathbf{x}_t from the expected behavior defined by f . An observation \mathbf{x}_t is classified as anomalous if its anomaly score S_t exceeds a predefined threshold τ . Thus, the set of detected anomalies is given by $\mathbf{A} = \{\mathbf{x}_t \mid S_t > \tau, t \in \{1, 2, \dots, T\}\}$.

According to [4], to model the dependence between a current time point and previous ones, we can define a time window W_t of length K at a given time t as follows:

$$W_t = \{\mathbf{x}_{t-K+1}, \dots, \mathbf{x}_{t-1}, \mathbf{x}_t\}. \quad (1)$$

It is then possible to transform the original time series $\mathbf{X} = \{\mathbf{x}_1, \mathbf{x}_2, \dots, \mathbf{x}_T\}$ into a sequence of windows $\mathbf{W} = \{W_1, \dots, W_T\}$ to be used as training input. Given a binary variable $y \in \{0, 1\}$, the goal of our anomaly detection problem is to assign to an unseen window $\widehat{W}_t, t > T$, a label y_t to indicate a detected anomaly at time t , i.e., $y_t = 1$ for an anomaly or $y_t = 0$ for normal behavior, based on the window's anomaly score. For the sake of simplicity and without loss of generality, we will use W to denote a training input window and \widehat{W} to denote an unseen input window.

3.2 Framework Overview

UniTS – see Figure 1 – is a versatile multi-task model featuring a unified network architecture. We exploit the original architecture to perform anomaly detection in time series data, as described hereafter.

Input Tokenization. UniTS employs a token-based approach to represent tasks and time series from various domains. It introduces two⁷ unique token types: i.e., *sample*, and *prompt*, each fulfilling a specific role in time series analysis.

- *Sample tokens.* The time series⁸ $\mathbf{X} \in \mathbb{R}^{T \times n}$. We split \mathbf{X} into patches along the time dimension via a non-overlapping patch size of k . Then, a linear layer projects each patch into an embedding vector of length d , obtaining sample tokens $z_{\mathbf{X}} \in \mathbb{R}^{\frac{T}{k} \times n \times d}$. $z_{\mathbf{X}}$ are added with learnable positional embeddings.

- *Prompt tokens.* They are defined as learnable embeddings $z_p \in \mathbb{R}^{p \times n \times d}$ where p is the number of tokens. These tokens incorporate the task UniTS needs to perform. Notice that, in Figure 1, we do not illustrate the prompt tokens proposed

⁷The original paper proposes three different tokens, among which also the task tokens, which we do not use in our scenario. We point the reader to [12] for more details on how task tokens are used.

⁸For simplicity, we assume that the entire time series \mathbf{X} has already been split into multiple windows \mathbf{W} . Therefore, at inference, one reconstructs a single window at a time.

in the original paper since we only exploit the *forecasting prompt* in our anomaly detection scenario. Nevertheless, for the sake of completeness, we invite the reader to visualize that these prompt tokens are prepended to the input series tokens as in Eq. (2).

$$z_{\text{Anomaly}} = [z_p, z_{\mathbf{X}}]_{\mathcal{T}} \in \mathbb{R}^{(p+\frac{T}{k}) \times n \times d}, \quad (2)$$

where $[*, *]_{\mathcal{T}}$ is the concatenation along the time axis.

UniTS modules. The model takes in input z_{Anomaly} and feeds it to N blocks of modified transformer architecture to handle heterogeneous multi-domain data with varying dynamics and the number of variables. We use the original UniTS architecture. In more detail, we use Time and Variable Multi-Head Self-Attention (MHSA) blocks, a Dynamic Feed-Forward Network (FFN), and gating modules. We refer the reader to the original paper’s appendix [12] for more detail on the transformer and tower modules.

- *Time and Variable MHSA.* As suggested in the original paper, we use a two-way self-attention for feature and time dimensions. This approach contrasts with previous methods that apply self-attention to either time or variable dimension but not to both dimensions. Time and variable self-attention effectively handle time series samples with various numbers of features n and different time lengths t .
- *Dynamic FFN.* The transformer block is modified by incorporating a dynamic operator into an FFN layer. This modification enables the FFN to capture dependencies between tokens, in contrast to the standard FFN, which processes embedding vectors on a point-wise basis.
- *Gating.* To mitigate interference in the latent representation space, gating modules are used after each layer. This module dynamically re-scales features in layer-wise latent spaces and promotes the stability of latent representations.
- *Tower.* This module transforms tokens into time points prediction results. Taking into consideration the generated sample tokens $\hat{z}_{\mathbf{X}}$, the tower module reconstructs the full time-series sample as in Eq. (3).

$$\hat{\mathbf{X}} = \text{Proj}(\text{MLP}(\hat{z}_{\mathbf{X}} + \text{DyLinear}(\hat{z}_{\mathbf{X}}))) \quad (3)$$

$$\begin{aligned} \text{DyLinear}(z_t, w) &= \mathbf{W}_{\text{Interp}} z_t \in \mathbb{R}^{l_{\text{out}} \times d} \\ \mathbf{W}_{\text{Interp}} &= \text{Interp}(w) \in \mathbb{R}^{l_{\text{in}} \times l_{\text{out}}}, \end{aligned} \quad (4)$$

where the MLP is composed of two linear layers with an activation layer in between, Proj is the unpatchify operation that transfers the embedding back to the time series patch; Interp is a bilinear interpolation to resize w from shape $w_{\text{in}} \times w_{\text{out}}$ to $l_{\text{in}} \times l_{\text{out}}$.

3.3 Fine-tuning UniTS for Abnormal Emotion Detection

UniTS was trained on a large, diverse dataset using a unified masked reconstruction scheme. This allows the model to learn general representations of temporal sequences and their underlying patterns, enhancing its generative and predictive task capabilities. Recall that UniTS is a foundational model in time series, and its training is executed on multiple tasks.

UniTS enables two different adaptation strategies for new datasets: i.e., whole model fine-tuning and prompt learning. The model weights are frozen in prompt learning, and only the prompt tokens are updated. According to [12], this performs similarly to fine-tuning at a lower computational cost. Nevertheless, because we want to demonstrate the capability of HR and HRV signals only to detect abnormal emotion detection via non-invasive wearable devices, we preprocess the datasets to obtain features at a low-frequency rate – see Sec. 4.2. This makes fine-tuning UniTS more “affordable” since we drastically reduce the sampling rate of the signals present in the dataset (e.g., from a sample of ECG of 700Hz to a transformed sample of HR/HRV of 0.1Hz). We follow [6] to reduce the sampling rate – this is also supported in Figure 3 – since we want to emulate the realness of how vital signals are measured with smartwatches while maintaining effective battery levels. Finally, note that we use 20 epochs and an exponential learning rate decay to fine-tune the model.

4 Experiments

4.1 Experimental Setup

Compared methods. We compare supervised UniTS and fine-tuned UniTS with various SoTA models for multivariate time-series anomaly detection. The models compared include TranAD[37], LSTM-NDT[19], CAEM[41], DAGMM[45], USAD[4], OmniAnomaly[35], MTAD-GAT[42], GDN[10], MAD-GAN[25], MSCRED[39],

HypAD[11], and TadGAN[13]. For these models, we adopted the hyperparameters as presented in their original papers and conducted a learning rate grid search using 5-fold cross-validation to ensure optimal performance.

Training UniTS. For fine-tuning UniTS, we used a window size of 5 and an embedding dimension of 128. These hyperparameters were selected based on an ablation study on the model. The datasets were divided into 80% training data and 20% validation data. All models were tested every 5 epochs since different convergence times may occur, and the best result for each fold was recorded and averaged to determine the optimal learning rate.

Fair comparisons and threshold settings. We systematically preprocessed our datasets to ensure consistency and comparability across different sources. From all datasets, we extracted Heart Rate (HR) and Heart Rate Variability (HRV) every 10 seconds using a sliding window approach based on the preceding 60 seconds of signal data from ECG and, when available, Blood Volume Pulse (BVP), which measure the volumetric change in blood circulation through the microvascular bed of tissue. BVP signals can be extracted non-invasively using photoplethysmography (PPG), a technique commonly integrated into smartwatches and other wearable devices. This capability is instrumental in stress detection and management, making wearable devices valuable in clinical and everyday settings.

Lastly, we use a threshold of the 3rd and 97th percentile to indicate anomalous data points: i.e., everything that is below the 3rd or above the 97th percentile is labeled as 1; otherwise, it is 0. Percentiles are calculated on the reconstruction errors.

4.2 Datasets

We use three widely adopted datasets for emotion detection:

DREAMER [20] is designed for emotion recognition via low-cost devices. It consists of EEG and ECG readings recorded from 23 participants. ECG signals were captured at a sampling rate of 256 Hz. Movie clips were used to stimulate different emotions in participants, and at the end of each clip, participants scored their self-assessment on a 5-point arousal, valence, and dominance scale. Here, we treat states with a valence of 1 as abnormal and the rest as normal.

MAHNOB-HCI [34] was collected using the Biosemi active II system with active electrodes to capture physiological signals, among others the ECG and EEG, from 27 participants at a sampling rate of 256 Hz. Participants were asked to record their emotional status after each trial, consisting of multimedia content stimulation. Here, we treat the states with a valence of 1 as abnormal and the rest of the emotional states as normal. For our experiments, we selected subsets of the dataset with recordings of at least 120 seconds and excluded those with incomplete tracks due to recording errors.

WESAD [33] has ECG and BVP signals from 15 participants at a rate of 700Hz extracted via a RespiBAN Professional 2 sensor worn on the chest. It contains four different emotional states. Here, we treat the stress state as abnormal and the rest as normal. The stress condition is obtained by exposing the subjects to the Tier Social Stress Test, which consists of public speaking and a mental arithmetic task.

(a) Comparison of different methods using HR and HRV extracted from ECG and BVP. Bold-faced values illustrate the best; underlined ones are the second best.

	DREAMER	HCI	WESAD (ECG)	WESAD (BVP)	AVG F1
LSTM-NDT	0.313	0.375	0.785	0.772	0.561 ± .218
OmniAnomaly	0.599	0.547	0.767	0.650	0.641 ± .081
CAE-M	0.658	0.530	0.801	0.590	0.645 ± .101
HypAD	0.650	0.643	0.815	0.567	0.669 ± .090
MTAD-GAT	0.536	0.742	0.857	0.719	0.714 ± .115
TranAD	0.617	0.623	0.837	<u>0.804</u>	0.720 ± .101
TadGAN	0.590	0.691	<u>0.864</u>	0.743	0.722 ± .099
GDN	0.713	0.580	0.858	0.802	0.738 ± .105
DAGMM	<u>0.743</u>	0.647	0.831	0.773	0.749 ± .067
USAD	0.730	0.660	0.830	0.797	0.754 ± .065
MAD-GAN	0.706	0.743	0.839	0.787	0.769 ± .050
MSCRED	0.675	<u>0.824</u>	0.876	0.775	0.788 ± .074
UniTS	0.869	0.878	0.834	0.856	0.859 ± .019

(b) P-values produced by the Dunn post-hoc test, where the control model is UniTS against the top-performing SoTA methods. We use a p-value of 5×10^{-2} to reject the null hypothesis.

UniTS	
MSCRED	2.813×10^{-2}
MAD-GAN	4.795×10^{-3}
USAD	6.839×10^{-3}
DAGMM	1.136×10^{-3}
GDN	5.146×10^{-3}

Table 2: Quantitative experiments of UniTS vs SoTA methods on three benchmarking datasets.

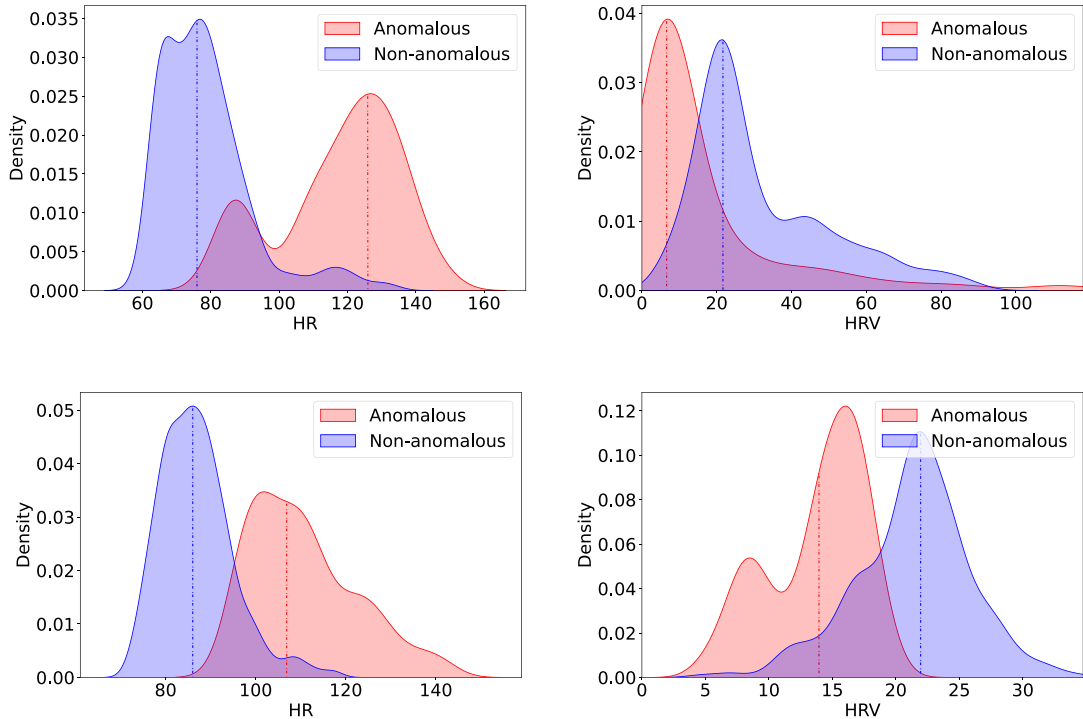


Figure 2: Density plots for HR and HRV on the test set for WESAD for ECG (up) and BVP (down) versions. We also show the means of the distributions with dashed lines.

4.3 Quantitative Results

UniTS surpasses SoTA anomaly detection systems and shows remarkable stability and robustness across datasets.

As shown in Table 2a, UniTS outperforms all the compared systems, achieving a considerable average improvement of 9% on the second-best – i.e., 16.95% on DREAMER, 6.55% on HCI, -4.79% on WESAD (ECG), and 6.47% on WESAD (BVP). We first conduct a Friedman Test on the top methods (UniTS, MSCRED, MAD-GAN, GDN, MTAD-GAT, TranAD) to show that UniTS has, statistically and significantly, the best performance across the board ($F = 12.174$, $p = .033 < .05$). Then, we perform a Dunn post-hoc test where the control anomaly detector is UniTS. The test suggests that UniTS is statistically and significantly different (better) across the board on average (see Table 2b). We also note that the competitive advantage of UniTS is lower in the WESAD (ECG) dataset. Several systems achieve more or less similar - and in some cases slightly better - performances. We argue this is because WESAD is the only dataset that explicitly includes stress among the classified emotions, while the other two datasets use dimensional models of emotions (arousal and valence), resulting in a nuanced and less "clear-cut" classification. In this simpler context, many systems perform much better. However, the difference between UniTS and the best competitors lies in the second significant digit after the decimal point. BVP can be noisy and contain many artefacts, which hardens extracting meaningful features from it [28]. Hence, in WESAD (BVP), the normal and anomalous data distribution is noised and does not respect that originally coming from the ECG – i.e., compare HR and HRV distributions in Figure 2, and notice the difference in scale in HRV coming from ECG and BVP – which we argue leads SoTA methods to underperform. Furthermore, UniTS, through its incorporated attention mechanism over the variates and the time axes, mitigates this phenomenon by giving less weight to noisy samples, maintaining high WESAD (BVP) performances.⁹

Overall, UniTS exhibits remarkably stable performance and higher robustness across all datasets and systems (std of only .019), resulting from being a universal model pre-trained on many diverse signals and tasks.

UniTS achieves performances from lightweight devices comparable to SoTA systems using more invasive and potentially accurate sensors. The only dataset collecting signals from ECG and smartwatch (BVP) is WESAD. Table 2a (columns 4 and 5) clearly shows that performance worsens with BPV for all systems except UniTS, which maintains similar F1 values for the ECG and BPV versions. This is a valuable result since, as discussed in Section 1, lightweight devices, such as bracelets and smartwatches, are less expensive and invasive, enabling seamless monitoring. Using non-invasive, wearable technology without sacrificing performance can expand stress-related research and applications.

⁹We verified that UniTS has an FPR of 0.028 in both versions of WESAD. Meanwhile, it reports an FNR of 0.118 in WESAD (ECG) and 0.073 in WESAD (BVP), suggesting that it is more capable of detecting the true anomalies (i.e., it has better recall).

Future studies can integrate these devices in various settings to gather continuous stress data, leading to personalized stress management programs, early intervention systems for mental health, and better well-being monitoring.

Lower sampling rates on lightweight devices makes performance plummet by $\sim 66\%$. Figure 3 shows the importance of the sampling rate on all datasets on ECG and BVP versions. Here, we illustrate the trend of average F1 scores of UniTS when the sampling interval increases from 10 to 60 seconds. The vital signals (i.e., HR and HRV) are sampled every k seconds to build the multivariate time series taken in input, with varying k . As expected, the longer the sampling interval, the less responsive the model becomes, resulting in a degradation of results. This phenomenon is even more visible when we extract the HR and HRV from BVP, having a drop of -66.12% passing from a 10 to a 60-second sampling rate.

This discrepancy highlights a critical consideration in the evolving landscape of wearable technology and continuous monitoring systems. While Malik et al. [29] provided foundational guidelines for HRV measurement, recommending high sampling rates of at least 200Hz for precise R-R interval¹⁰ detection from ECG and 2-to-5-minutes for BVP, our empirical findings suggest that for real-time HRV analysis, using BVP signals, the sampling intervals must be significantly shorter to maintain model performance. We suggest a re-evaluation of the balance between device convenience and performance. For applications requiring high precision, such as medical diagnostics or performance monitoring in athletes, adhering to more frequent sampling intervals appears imperative. Therefore, our study advocates for a nuanced approach, where the selection of sampling intervals is tailored to the specific requirements of the use case, ensuring that the integrity of physiological data is not compromised by the constraints of the monitoring device.

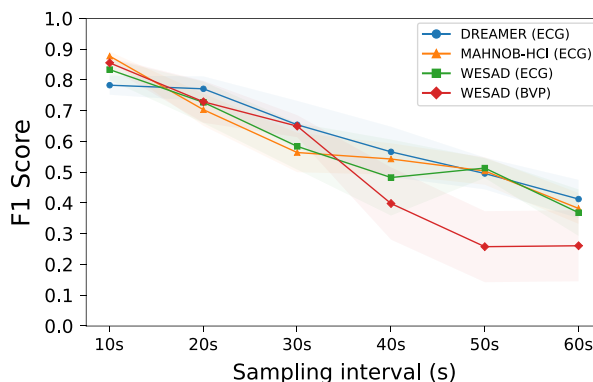


Figure 3: Performance degradation of F1 score across different sampling intervals using the UniTS on all the datasets.

4.4 Qualitative Results

Casting the problem as one of anomaly detection enhances explainability. Anomaly detection begins by establishing a model of "normal" behavior based on the monitored signals, and next, it detects deviations from this normality. This helps clinicians understand the baseline from which deviations are identified and aligns better with medical professionals' needs and practical constraints. First, clinicians are usually more interested in identifying and investigating abnormalities rather than confirming the norm. Anomaly detection systems align with doctors' diagnostic workflow by focusing on detecting deviations from the norm. Secondly, these models provide significant benefits for precision medicine and personalization due to their ability to identify unique patient profiles and adapt to new data continuously [30]. Furthermore, in the case of multiple monitored signals, the model should highlight which ones are more indicative of stress [3]. In Figure 4, we aim to support doctors in identifying which signals contributed the most in detecting anomalies. Here, we depict the contribution probability based on the reconstruction error of each signal – i.e., HR (up) and HRV (middle) – in determining anomalies. The more opaque the shade of each bar in the plot, the more likely an anomaly will occur. Notice how the opacity of the probabilities increases when there is an abrupt trend change in one (or both) of the signals, which aligns with the red areas depicting the detection of an anomaly. One can think of the transparency of each bar as a visual uncertainty of the model. Therefore, the more opaque the bars are, the more certain the model is that there is an anomaly in that particular time frame. Meanwhile, when the bars are transparent, they may indicate two things: either the model is uncertain, or the data points therein are normal. To this end, we integrate the contribution probability with detecting anomalies in the raw signals. Additionally, we invite the reader to notice the different transparency levels within the time frame where an anomaly is detected. This phenomenon is expected as not all types of anomalies (gradual vs. abrupt) are detected with the same confidence. Interestingly, in this scenario, badly reconstructing HR pushes the model to be more confident about an anomaly occurring – see the middle portion of the third row in Figure 4. Contrarily, even if UniTS cannot effectively reconstruct HRV, it does not lead to detecting anomalies – e.g., notice the more transparent tail-ends of the probabilities plot. By exploiting these types of explicit and inherently interpretable visualizations – i.e., the contribution probability is estimated via the reconstruction error – doctors can interpret which signal guides the prediction of an anomaly during inference and intervene accordingly. Finally, this type of analysis can be used to debug if the monitoring system functions correctly. For instance, if the

¹⁰<https://www.sciencedirect.com/topics/nursing-and-health-professions/rr-interval>



Figure 4: HR (up) and HRV (middle) contribution in WESAD (BVP) during inference time. Red-shaded areas depict the reported anomalies. The lower bar plot illustrates the contribution probabilities based on the reconstruction error of each signal. The more transparent the contribution, the lower the chances of the signals being considered anomalous; the more opaque the contributions are, the more the chances of the signals being anomalous. Note that the transparency can be seen as visual uncertainty about the data point at a particular time step.

contribution probability bars are opaque, yet the system does not report an anomaly, there might be something wrong with the current monitoring setup.

5 Conclusion

This is the first study to employ a universal time series model, UniTS, to support the seamless monitoring of physiological signals. We have demonstrated that UniTS significantly outperforms state-of-the-art machine learning models for stress detection. Furthermore, it performs similarly when using invasive monitoring devices, such as the ECG, and lightweight, such as a smartwatch or bracelet. This equivalence is valid as long as the sampling frequency is sufficiently high but still well within the reach of existing devices, even less expensive ones. Monitoring patients' disease progression via lightweight devices has numerous advantages, including increased patient comfort and compliance, continuous and real-time monitoring, reduced healthcare costs, increased patient independence, personalized care, improved remote management of patients, and better health outcomes through early intervention.

We acknowledge that this study also has limitations. For example, the study compares HR and HRV extracted from a smartwatch and ECG, partly due to the wider availability of benchmark datasets for this type of signal. In the future, we plan to extend our experiments to a wider variety of physiological signals that are both detectable by lightweight devices and relevant to studying mental states, such as physical activity and sleep quality. We also intend to go beyond stress monitoring to include the observation of other signals of physical and cognitive decline, such as daily activity routines and other actigraphy data, as well as contextual factors. Note that UniTS (see Section 3) by design allows the integration of time series of different types and lengths. However, the obstacle to this type of experiment is rather the absence of datasets that collect, for each monitored patient, multiple signals from multiple devices in naturalistic settings. To overcome the shortage of available datasets, we are collecting, in the context of the Regional project @HOME, a variety of physiological, behavioral, and environmental signals for a cohort of 10 patients monitored in their homes.

Acknowledgements

This work was supported by a grant from Lazio Region, FESR Lazio 2021-2027, project @HOME (# F89J23001050007 CUP B83C23006240002).

References

- [1] Joong Woo Ahn, Yunseo Ku, and Hee Chan Kim. A novel wearable eeg and ecg recording system for stress assessment. *Sensors*, 19(9):1991, 2019.
- [2] Abdullah A Al-Atawi, Saleh Alyahyan, Mohammed Naif Alatawi, Tariq Sadad, Tareq Manzoor, Muhammad Farooq-i Azam, and Zeashan Hameed Khan. Stress monitoring using machine learning, iot and wearable sensors. *Sensors*, 23(21):8875, 2023.
- [3] H Ceren Ates, Cihan Ates, and Can Dincer. Stress monitoring with wearable technology and ai. *Nature Electronics*, pages 1–2, 2024.
- [4] Julien Audibert, Pietro Michiardi, Frédéric Guyard, Sébastien Marti, and Maria A Zuluaga. Usad: Unsupervised anomaly detection on multivariate time series. In *Proceedings of the 26th ACM SIGKDD international conference on knowledge discovery & data mining*, pages 3395–3404, 2020.
- [5] Seif-Eddine Benkabou, Khalid Benabdeslem, Vivien Kraus, Kilian Bourhis, and Bruno Canitia. Local anomaly detection for multivariate time series by temporal dependency based on poisson model. *IEEE Transactions on Neural Networks and Learning Systems*, 2021.
- [6] Gerald Bieber, Thomas Kirste, and Michael Gaede. Low sampling rate for physical activity recognition. In *Proceedings of the 7th International Conference on PErvasive Technologies Related to Assistive Environments, PETRA '14*, New York, NY, USA, 2014. Association for Computing Machinery.
- [7] Aaron Frederick Bulagang, James Mountstephens, and Jason Teo. Multiclass emotion prediction using heart rate and virtual reality stimuli. *Journal of Big Data*, 8:1–12, 2021.
- [8] Yekta Said Can, Niaz Chalabianloo, Deniz Ekiz, and Cem Ersoy. Continuous stress detection using wearable sensors in real life: Algorithmic programming contest case study. *Sensors*, 19(8):1849, 2019.
- [9] Janette Cardoso, Robert Valette, and Didier Dubois. Fuzzy petri nets: an overview. *IFAC Proceedings Volumes*, 29(1):4866–4871, 1996.
- [10] Ailin Deng and Bryan Hooi. Graph neural network-based anomaly detection in multivariate time series. In *Proceedings of the AAAI conference on artificial intelligence*, volume 35, pages 4027–4035, 2021.
- [11] Alessandro Flaborea, Bardh Prenkaj, Bharti Munjal, Marco Aurelio Sterpa, Dario Aragona, Luca Podo, and Fabio Galasso. Are we certain it’s anomalous? In *Proceedings of the IEEE/CVF Conference on Computer Vision and Pattern Recognition*, pages 2896–2906, 2023.
- [12] Shanghua Gao, Teddy Koker, Owen Queen, Thomas Hartvigsen, Theodoros Tsiligkaridis, and Marinka Zitnik. Units: Building a unified time series model. *arXiv preprint arXiv:2403.00131*, 2024.
- [13] Alexander Geiger, Dongyu Liu, Sarah Alnegheimish, Alfredo Cuesta-Infante, and Kalyan Veeramachaneni. Tadgan: Time series anomaly detection using generative adversarial networks. In *2020 IEEE International Conference on Big Data (Big Data)*, pages 33–43. IEEE, 2020.
- [14] Adnan Ghaderi, Javad Frounchi, and Alireza Farnam. Machine learning-based signal processing using physiological signals for stress detection. In *2015 22nd Iranian Conference on Biomedical Engineering (ICBME)*, pages 93–98, 2015.
- [15] Martin Gjoreski, Mitja Luštrek, Matjaž Gams, and Hristijan Gjoreski. Monitoring stress with a wrist device using context. *Journal of biomedical informatics*, 73:159–170, 2017.
- [16] Han-Wen Guo, Yu-Shun Huang, Chien-Hung Lin, Jen-Chien Chien, Koichi Haraikawa, and Jiann-Shing Shieh. Heart rate variability signal features for emotion recognition by using principal component analysis and support vectors machine. In *2016 IEEE 16th international conference on bioinformatics and bioengineering (BIBE)*, pages 274–277. IEEE, 2016.
- [17] Lutfi Hakim, Adhi Dharma Wibawa, Evi Septiana Pane, and Mauridhi Hery Purnomo. Emotion recognition in elderly based on spo 2 and pulse rate signals using support vector machine. In *2018 IEEE/ACIS 17th International Conference on Computer and Information Science (ICIS)*, pages 474–479. IEEE, 2018.
- [18] Kenneth M Heilman and Stephen E Nadeau. Emotional and neuropsychiatric disorders associated with alzheimer’s disease. *Neurotherapeutics*, 19(1):99–116, 2023.

- [19] Kyle Hundman, Valentino Constantinou, Christopher Laporte, Ian Colwell, and Tom Soderstrom. Detecting spacecraft anomalies using lstms and nonparametric dynamic thresholding. In *Proceedings of the 24th ACM SIGKDD international conference on knowledge discovery & data mining*, pages 387–395, 2018.
- [20] Stamos Katsigiannis and Naeem Ramzan. Dreamer: A database for emotion recognition through eeg and ecg signals from wireless low-cost off-the-shelf devices. *IEEE journal of biomedical and health informatics*, 22(1):98–107, 2017.
- [21] Jonghwa Kim and Elisabeth André. Emotion recognition based on physiological changes in music listening. *IEEE transactions on pattern analysis and machine intelligence*, 30(12):2067–2083, 2008.
- [22] Emilija Knezevic, Katarina Nenic, Vladislav Milanovic, and Nebojsa Nick Knezevic. The role of cortisol in chronic stress, neurodegenerative diseases, and psychological disorders. *Cells*, 12(23), 2023.
- [23] Robert Kraut, Han Li, and Haiyi Zhu. Mental health during the covid-19 pandemic: Impacts of disease, social isolation, and financial stressors. *PLOS ONE*, 17:e0277562, 11 2022.
- [24] Hindra Kurniawan, Alexandr V. Maslov, and Mykola Pechenizkiy. Stress detection from speech and galvanic skin response signals. In *Proceedings of the 26th IEEE International Symposium on Computer-Based Medical Systems*, pages 209–214, 2013.
- [25] Dan Li, Dacheng Chen, Lei Shi, Baihong Jin, Jonathan Goh, and See-Kiong Ng. Mad-gan: Multivariate anomaly detection for time series data with generative adversarial networks. In *ICANN*, 2019.
- [26] Hailun Lian, Cheng Lu, Sunan Li, Yan Zhao, Chuangao Tang, and Yuan Zong. A survey of deep learning-based multimodal emotion recognition: Speech, text, and face. *Entropy*, 25(10), 2023.
- [27] Qiang Lin, Tongtong Li, P Mohamed Shakeel, and R Dinesh Jackson Samuel. Advanced artificial intelligence in heart rate and blood pressure monitoring for stress management. *Journal of Ambient Intelligence and Humanized Computing*, 12:3329–3340, 2021.
- [28] Simon Luo, Jianlong Zhou, Henry Been-Lirn Duh, and Fang Chen. Bvp feature signal analysis for intelligent user interface. In *Proceedings of the 2017 CHI Conference Extended Abstracts on Human Factors in Computing Systems*, CHI EA '17, page 1861–1868, New York, NY, USA, 2017. Association for Computing Machinery.
- [29] Marek Malik, J. Thomas Bigger, A. John Camm, Robert E. Kleiger, Alberto Malliani, Arthur J. Moss, and Peter J. Schwartz. Heart rate variability: Standards of measurement, physiological interpretation, and clinical use. *European Heart Journal*, 17(3):354–381, 03 1996.
- [30] Parvaneh Parvin, Stefano Chessa, Maurits Kaptein, and Fabio Paternò. Personalized real-time anomaly detection and health feedback for older adults. *Journal of Ambient Intelligence and Smart Environments*, 11:453–469, 09 2019.
- [31] Bardh Prenkaj and Paola Velardi. Unsupervised detection of behavioural drifts with dynamic clustering and trajectory analysis. *IEEE Transactions on Knowledge and Data Engineering*, 2023.
- [32] Akane Sano and Rosalind W. Picard. Stress recognition using wearable sensors and mobile phones. In *2013 Humaine Association Conference on Affective Computing and Intelligent Interaction*, pages 671–676, 2013.
- [33] Philip Schmidt, Attila Reiss, Robert Duerichen, Claus Marberger, and Kristof Van Laerhoven. Introducing wesad, a multimodal dataset for wearable stress and affect detection. In *Proceedings of the 20th ACM international conference on multimodal interaction*, pages 400–408, 2018.
- [34] Mohammad Soleymani, Jeroen Lichtenauer, Thierry Pun, and Maja Pantic. A multimodal database for affect recognition and implicit tagging. *IEEE transactions on affective computing*, 3(1):42–55, 2011.
- [35] Ya Su, Youjian Zhao, Chenhao Niu, Rong Liu, Wei Sun, and Dan Pei. Robust anomaly detection for multivariate time series through stochastic recurrent neural network. In *Proceedings of the 25th ACM SIGKDD international conference on knowledge discovery & data mining*, pages 2828–2837, 2019.
- [36] Georgios Taskasaplidis, Dimitris Fotiadis, and Panagiotis Bamidis. Review of stress detection methods using wearable sensors. *IEEE Access*, PP:1–1, 01 2024.
- [37] Shreshth Tuli, Giuliano Casale, and Nicholas R. Jennings. Tranad: Deep transformer networks for anomaly detection in multivariate time series data. *Proc. VLDB Endow.*, 15(6):1201–1214, 2022.
- [38] Zhiwei Wang, Zhengzhang Chen, Jingchao Ni, Hui Liu, Haifeng Chen, and Jiliang Tang. Multi-scale one-class recurrent neural networks for discrete event sequence anomaly detection. In *The 27th ACM SIGKDD Conference on Knowledge Discovery and Data Mining*, pages 3726–3734. ACM, 2021.

- [39] Chuxu Zhang, Dongjin Song, Yuncong Chen, Xinyang Feng, Cristian Lumezanu, Wei Cheng, Jingchao Ni, Bo Zong, Haifeng Chen, and Nitesh V Chawla. A deep neural network for unsupervised anomaly detection and diagnosis in multivariate time series data. In *Proceedings of the AAAI conference on artificial intelligence*, volume 33, pages 1409–1416, 2019.
- [40] Jing Zhang, Hang Yin, Jiayu Zhang, Gang Yang, Jing Qin, and Ling He. Real-time mental stress detection using multimodality expressions with a deep learning framework. *Frontiers in Neuroscience*, 16, 2022.
- [41] Yuxin Zhang, Yiqiang Chen, Jindong Wang, and Zhiwen Pan. Unsupervised deep anomaly detection for multi-sensor time-series signals. *IEEE Transactions on Knowledge and Data Engineering*, 35(2):2118–2132, 2021.
- [42] Hang Zhao, Yujing Wang, Juanyong Duan, Congrui Huang, Defu Cao, Yunhai Tong, Bixiong Xu, Jing Bai, Jie Tong, and Qi Zhang. Multivariate time-series anomaly detection via graph attention network. In *2020 IEEE International Conference on Data Mining (ICDM)*, pages 841–850. IEEE, 2020.
- [43] Bin Zhou, Shenghua Liu, Bryan Hooi, Xueqi Cheng, and Jing Ye. Beatgan: Anomalous rhythm detection using adversarially generated time series. In *Proceedings of the Twenty-Eighth International Joint Conference on Artificial Intelligence, IJCAI-19*, pages 4433–4439. International Joint Conferences on Artificial Intelligence Organization, 7 2019.
- [44] Jiaqi Zhu, Fang Deng, Jiachen Zhao, Daoming Liu, and Jie Chen. Uaed: Unsupervised abnormal emotion detection network based on wearable mobile device. *IEEE Transactions on Network Science and Engineering*, 10(6):3682–3696, 2023.
- [45] Bo Zong, Qi Song, Martin Renqiang Min, Wei Cheng, Cristian Lumezanu, Daeki Cho, and Haifeng Chen. Deep autoencoding gaussian mixture model for unsupervised anomaly detection. In *International conference on learning representations*, 2018.